Sensitivity of the WRF Model to Advection and Diffusion Schemes for Simulation of Heavy Rainfall along the Baiu Front

Hiroyuki Kusaka[1], Andrew Crook[2], Jason C. Knievel[2], and Jimy Dudhia[2]
[1]*Central Research Institute of Electric Power Industry, Abiko, Japan*
[2]*National Center for Atmospheric Research, Boulder, CO, USA*

Abstract

A series of numerical experiments were conducted to investigate the sensitivity of the WRF Model to the advection scheme. The differences in the simulated results between third- and fifth-order schemes are not large, however the vertical velocity field of the former is somewhat smoother. On the other hand, fourth- and sixth-order schemes easily produce grid-scale computational noise, although the time step is set to be smaller than the recommended one. Artificial second-order diffusion damps the noise, however it negates the advantage of the high-order advection scheme. Explicit fourth-order diffusion damps the noise, however it smoothes the field more than the inherent, implicit diffusion in the third-order scheme. Contrary to this, explicit sixth-order diffusion damps noise, but maintains detailed structure and high energy spectral density of the vertical velocity. We recommend the fifth-order upwind scheme for use in the WRF Model.

1. Introduction

The Weather Research and Forecasting (WRF) model, which is a new compressible, non-hydrostatic model, has been developed by collaboration among the National Center for Atmospheric Research (NCAR), National Center for Environmental Prediction (NCEP), Forecast System Laboratory of the NOAA (NOAA/FSL), and Air Force Weather Agency (AFWA), etc. The Advanced Research core version of this model is designed as the next generation model after the PSU/NCAR-MM5 (Dudhia 1993), which has been widely used all over the world. One of the big differences between WRF and MM5 is that the dynamical core of WRF uses high-order accurate discretization schemes for time and space: third-order Runge-Kutta scheme for the time integration, and second- to sixth-order schemes for the advection terms (Skamarock et al. 2005). Another difference is that the latest official release version of the WRF does not yet include explicit numerical diffusion. Many current MM5 users will use WRF in the near future. Thus, we need to investigate the WRF advection schemes and numerical filters.

Most of the numerical studies on the spatial discretization schemes have been investigated for idealized, conditions using a simple advection model or NWP model (e.g., Durran 1999; Ferziger and Peric 2002; Wicker and Skamarock 2002; Klemp and Skamarock 2004). Takemi and Rotunno (2003) investigated the effects of fourth-order diffusion on the development of linearly-organized moist convection and found that it has a significantly negative impact on the simulations. Skamarock (2004) compared the differences in the spectral density of kinetic energy within the free atmosphere between the fifth-order upwind scheme and second-order centered scheme with second- or fourth-order diffusion, and pointed out the second-order centered schemes have lower effective resolution. However, the sensitivity of WRF to the advection and diffusion schemes has not been systematically investigated. In this study, we will systematically investigate the sensitivity of WRF to the third- to sixth-order horizontal advection schemes and the second- to sixth-order numerical diffusion for the simulation of heavy rainfall along the Baiu front.

2. Experimental design

The Baiu front extended from the Sea of Japan to the Pacific Ocean, and heavy rainfalls occurred along the front on July 13th 2004 (Fig. 1). At 0900 JST, a convective line was well developed and produced a banded heavy rainfall exceeding 100 mm per three-hours (Figs. 2 and 3). Afterward, the heavy rainfalls gradually dissipated. In this study, we will conduct a series of numerical experiments of the heavy rainfall. We used two nested domains for all numerical experiments. The first (outer) domain is 3600 km by 3360 km in the horizontal direction, which includes Japan, Taiwan, and southern part of Sakhalin. This area is slightly smaller than that of Fig. 1. The second (inner) domain is 1320 km by 1200 km. Horizontal grid spacing is 12 km and 4 km for the domains 1 and 2, respectively. The model top is 50 hPa, and 31 sigma levels are used in the vertical. WRF was run for 24 hours beginning at 2100 JST July 12th 2004. Details of the configurations are summarized in Appendices 1. Experimental cases are summarized in Table 1.

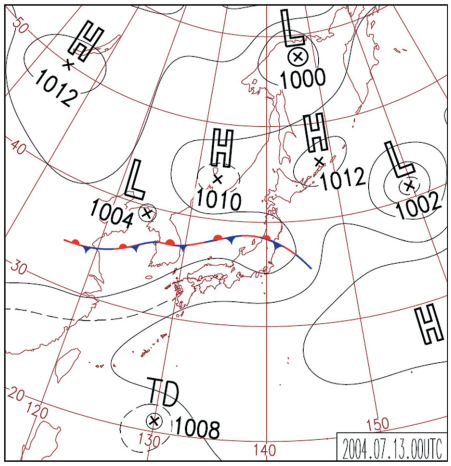

Fig. 1. Surface Weather Chart on 0900 Japan Standard Time (JST) July 13th 2004.

Corresponding author: Hiroyuki Kusaka, Fluid Dynamics Sector, Central Research Institute of Electric Power Industry, Abiko 270-1194, Japan. E-mail: h-kusaka@criepi.denken.or.jp.
©2005, the Meteorological Society of Japan.

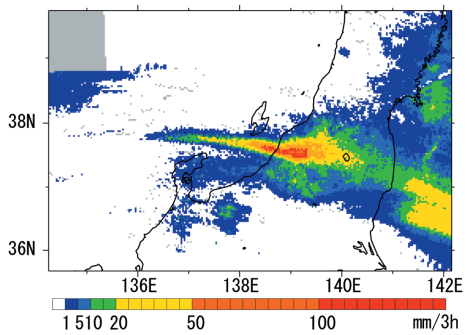

Fig. 2. Three-hourly accumulated precipitation at 0900 JST July 13th 2004. Radar AMeDAS data.

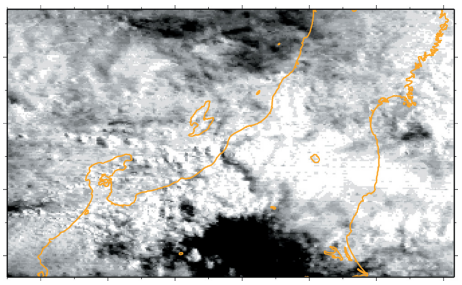

Fig. 3. Satellite GOES-9 visible image at 0900 JST July 13th, 2004.

3. Results

3.1 Sensitivity to advection schemes

Figure 4 shows three-hourly accumulated precipitation at 0600 JST from WRF using a fifth-order upwind scheme. In this case, the banded heavy rainfall is simulated around the Niigata area. However, the regional rainfalls exceeding 100 mm per three hours appear and disappear earlier than the observation. Figure 5 illustrates the 850hPa vertical velocity at 0600 JST from the numerical experiments, Cases 3S, 4S, 5S, and 6S. The region of strong upward velocity is consistent with that of the heavy rainfall in Case 5S (Figs. 4 and 5c). The velocity fields are similar to each other in Cases 3S and 5S. However the field of the former is somewhat smoother because the implicit diffusion works more strongly. On the other hand, the results from Cases 4S and 6S are very different from Cases 3S and 5S. In Cases 4S and 6S, the grid-scale upward and downward wind are seen. At least, part of this noise may be computational, which is a numerical energy cascade to finer scales.

Table 1. Experimental cases. For Cases 4F and 6F, explicit diffusion was added by the authors.

Case	Advection Scheme	Numerical Diffusion
3S	3rd-order upwind	4th-order (Implicit)
4S	4th-order centered	
5S	5th-order upwind	6th-order (Implicit)
6S	6th-order centered	
4C	4th-order centered	2nd-order (Explicit)
6C	6th-order centered	2nd-order (Explicit)
4F	4th-order centered	4th-order (Explicit)
6F	6th-order centered	6th-order (Explicit)

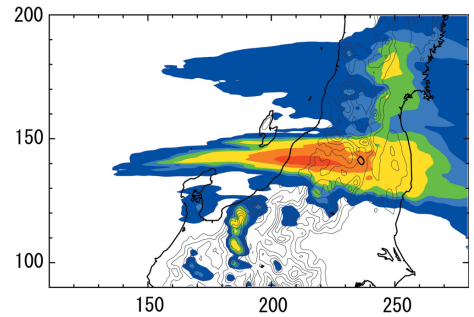

Fig. 4. Three-hourly accumulated precipitation at 0600 JST from Case 5S. Color bar is same as that of Fig. 2. Axis is grid point of domain 2.

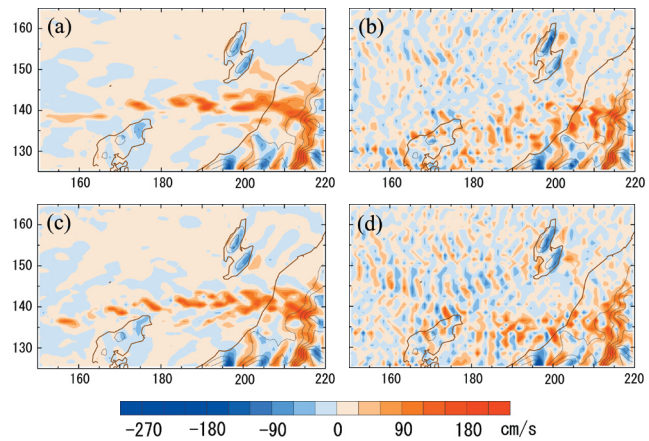

Fig. 5. Vertical velocity at 850hPa at 0600 JST. (a) Case 3S, (b) Case 4S, (c) Case 5S, and (d) Case 6S. Axis is grid point of domain 2.

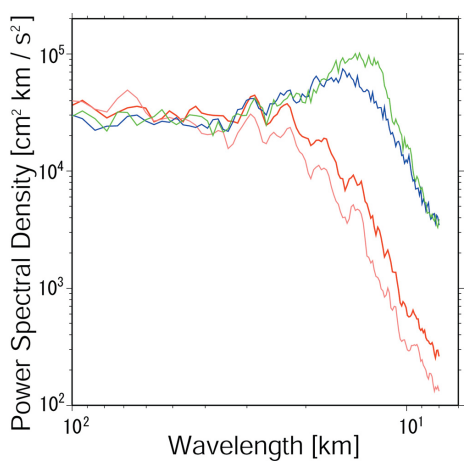

Fig. 6. Power spectral density of 850hPa vertical velocity computed from Cases 3S (pink), 4S (blue), 5S (red), and 6S (green). Data in the Fig. 5 and its east and west regions (from 32 to 288) are used.

Power spectral densities in the along-line (x) direction to the front were computed, referring to Takemi and Rotunno (2003). Figure 6 shows the differences among the advection schemes. In Cases 4S and 6S, there

is a buildup of the energy at short wavelengths, which is unnatural (Takemi and Rotunno 2003). Additionally, higher order spatial discretization schemes produce more energy in this wavelength band when the even-order centered-schemes are set up for the simulation of this heavy rainfall event. In contrast to this, there is no unnatural buildup of energy in Cases 3S and 5S. In the WRF, each of the upwind schemes is equivalent to a centered scheme of the next higher order plus a diffusion term of the next higher order with a coefficient proportional to the Courant number (Appendices 2). From this, we consider the implicit numerical diffusion prevents the growth of the numerical instability, removing the energy from the shortest spatial scale. The shapes of the spectra are similar between Cases 3S and 5S, but Case 5S has more energy for wavelengths shorter than ten times the horizontal grid spacing. These results indicate that the fifth-order scheme more clearly simulates the region of the strong vertical velocity than the third-order scheme because of weaker implicit numerical diffusion.

3.2 Sensitivity to numerical diffusion

To eliminate the undesirable properties of even-order schemes, some users may want to try another option of the horizontal diffusion term, which sets the horizontal diffusion coefficient to be constant. This is the easiest approach at present, although it is almost equivalent to adding the second-order artificial diffusion. Another solution is to add a fourth-order numerical diffusion to the dynamics with the fourth-order centered scheme, which is a standard approach to reduce noise. In the present experiments, we set the non-dimensional diffusion coefficient to 5.0×10^{-3} for the approaches using second- and fourth-order numerical diffusion. This is the value used in MM5. For the dynamics with the sixth-order centered scheme, we added the sixth-order numerical diffusion (Appendices 3). The coefficient in the sixth-order numerical diffusion is set to be the 1/4 of the fourth-order one to insure that both diffusions will damp a $2\Delta x$ wave at the same rate (Durran 1999).

Comparing the results from Cases 4S and 4C, the standard coefficient in the horizontal diffusion term damps the grid-scale noise (Fig. 7a, and Figs. 6 and 8). However the approach damps longer wavelengths, and thus negates the advantage of the higher-order advection scheme. Perhaps due to the smoothed field, the area of heavy rainfall from Case 4C is smaller than that of Case 3S (Table 2). In contrast to this, Case 4F maintains detail upward velocity fields (Fig. 7b).

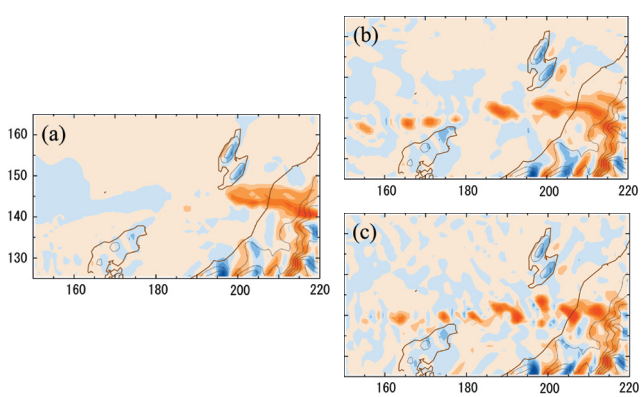

Fig. 7. Same as Fig. 5, but for (a) Case 4C, (b) Case 4F, and (c) Case 6F.

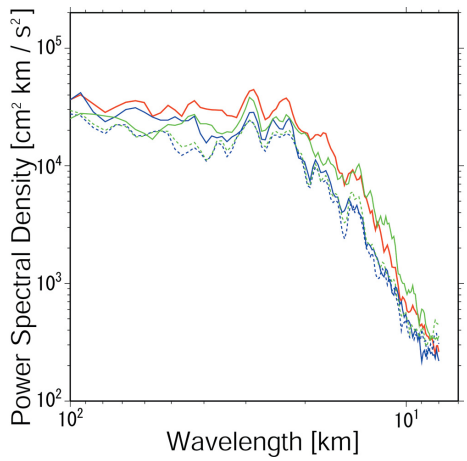

Fig. 8. Same as Fig. 6, except for Cases 4C (blue broken), 6C (green broken), 4F (blue solid), 6F (green solid), and 5S (red solid).

Table 2. Number of grid points of precipitation exceeding 20 mm per 3-hours in the domain of Fig. 4.

	03–06 JST	06–09 JST	09–12 JST
Case 3S	1479	1319	651
Case 5S	1648	1440	699
Case 4C	1194	1113	512
Case 6C	1202	1122	548
Case 4F	1404	1252	608
Case 6F	1545	1423	635

However, the fourth-order explicit numerical diffusion is slightly stronger than implicit ones (Figs. 5c and 7b, and Figs. 6 and 8).

On the other hand, Case 6F holds more detailed structure and damps noise. Comparison of the power spectral density between Cases 4F and 6F clearly shows that the energy of the short wavelengths is much less when the fourth-order numerical diffusion is used, even though the damping rate on the $2\Delta x$ is the same (Fig. 8). This indicates that the scale selectivity of the sixth-order numerical diffusion works well. Comparing the Case 6F to Case 5S, at low wavelengths, the two cases are very similar to each other but are different from the other cases in Fig. 8, because the other cases have less power at the right end of the figure. At large wavelengths, Case 6F has a little less power than does Case 5S. It is hard to say one is better than the other, but the sixth-order diffusion has an additional parameter to specify. Therefore, we recommend the fifth-order upwind scheme.

4. Conclusions

We first confirmed that WRF simulated well the observed banded heavy rainfall along the Baiu front, although the heavy rainfall appeared and disappeared earlier than the observation. Second, a series of numerical experiments were conducted to investigate the sensitivity of WRF to the advection scheme.

(1) The vertical velocity field from Case 3S is similar to that from Case 5S, however the former is somewhat smoother.

(2) On the other hand, Cases 4S and 6S easily produce grid-scale computational noise in the present simula-

tion.
(3) Cases 4C and 6C damp the noise, however the diffusion negates the advantage of the higher-order scheme.
(4) Case 4F damps the noise, however the smoothing is slightly stronger than Cases 3S and 5S.
(5) Case 6F damps the noise and holds more detailed structure and greater power spectral energy density of the vertical velocity than Case 4F.
(6) We here recommend the fifth-order upwind scheme for use in the WRF Model.

These results will be useful when doing simulations using WRF and the other NWP models.

References

Dudhia, J., 1993: A nonhydrostatic version of the Penn State/NCAR mesoscale model: Validation tests and simulation of an Atlantic cyclone and cold front. *Mon. Wea. Rev.*, **121**, 1493–1513.

Durran, D. R., 1999: *Numerical methods for wave equations in geophysical fluid dynamics*, Springer-Verlag, 465 pp.

Ferziger, J. H., and M. Peric, 2002: *Computational methods for fluid dynamics*, Springer-Verlag, 400 pp.

Klemp, J. B., and W. C. Skamarock, 2004: Model numerics for convective-storm simulation, 117–137. *Atmospheric turbulence and mesoscale meteorology*, Cambridge University Press, 280 pp. (ed) Fedorovich, E., R. Rutunno, and B. Stevens.

Knievel, J. C., G. H. Bryan, and J. P. Hacker, 2005: The utility of 6th-order, monotonic, numerical diffusion in the Advanced Research WRF Model. Preprints, *Joint WRF/MM5 Users' Workshop*, Boulder, CO, USA, NCAR, 27–30 June 2005, CD-ROM.

Skamarock, W. C., 2004: Evaluating mesoscale NWP models using kinetic energy spectra. *Mon. Wea. Rev.*, **132**, 3019–3032.

Skamarock, W. C., J. B. Klemp, J. Dudhia, D. O. Gill, D. M. Barker, W. Wang, and J. G. Powers, 2005: A description of the advanced research WRF version 2. NCAR/TN-468+STR, 88 pp.

Takemi, T., and R. Rotunno, 2003: The effects of subgrid model mixing and numerical filtering in simulations of mesoscale cloud systems. *Mon. Wea. Rev.*, **131**, 2085–2101.

Wiker, L. J., and W. C. Skamarock, 2002: Time splitting methods for elastic models using forward time schemes. *Mon. Wea. Rev.*, **130**, 2088–2097.

Appendices

1. Model configuration

Table A1. Configuration of the WRF Model version 2.0.3.1 used in the present study. Time step satisfies the CFL condition.

Dynamics	Advanced research core with mass coordinate system
Time integration	Time-split method using 3rd-order Runge-Kutta scheme with smaller time step for acoustic and gravity wave modes
Spatial discritization	Table 1 (horizontal) 3rd-order upwind (vertical)
Land surface	Noah-LSM
Planetary boundary layer	MRF
Horizontal diffusion	2D-Smagorinsky or constant
Shortwave radiation	Dudhia
Longwave radiation	RRTM
Cloud microphysics	Lin
Cumulus parameterization	Kain-Fritch (d01)
Time step	60 sec (d01), 20 sec (d02)
Initial and boundary conditions	NCEP Final Analysis Data

2. Spatial discritization scheme for advection term

Finite difference representation for the flux form of the scalar advection term in one dimension is written as:

$$\frac{\partial(U\phi)}{\partial x} = \frac{F_{i+1/2}-F_{i-1/2}}{\Delta x}, \tag{A1}$$

where, F_i is the flux at i grid. The fourth- and sixth-order accurate schemes to the derivatives on the right-hand side of (1) are written on the Arakawa-C staggered grid as (Skamarock et al. 2005):

$$F^{4\mathrm{th}}_{i-1/2} = \frac{U_{i-1/2}}{12}[7(\phi_i+\phi_{i-1})-(\phi_{i+1}+\phi_{i-2})], \tag{A2}$$

$$F^{6\mathrm{th}}_{i-1/2} = \frac{U_{i-1/2}}{60}[37(\phi_i+\phi_{i-1})-8(\phi_{i+1}+\phi_{i-2}) + (\phi_{i+2}+\phi_{i-3})], \tag{A3}$$

and the third- and fifth-order schemes are written as:

$$F^{3\mathrm{rd}}_{i-1/2} = F^{4\mathrm{th}}_{i-1/2} - \frac{|U_{i-1/2}|}{12}[3(\phi_i-\phi_{i-1})-(\phi_{i+1}-\phi_{i-2})], \tag{A4}$$

$$F^{5\mathrm{th}}_{i-1/2} = F^{6\mathrm{th}}_{i-1/2} - \frac{|U_{i-1/2}|}{60}[10(\phi_i-\phi_{i-1})-5(\phi_{i+1}-\phi_{i-2}) + (\phi_{i+2}-\phi_{i-3})], \tag{A5}$$

The even-order schemes are centered-biased and the odd-order schemes are upwind-biased. For constant flow, it can be shown that each of the upwind schemes is equivalent to a centered scheme of the next higher order plus a diffusion term of the next higher order with a coefficient proportional to the Courant number. Thus, the equations (A2)-(A5) are computed in the same way.

3. Explicit numerical diffusion

Fourth- and sixth-order numerical diffusions, D_4 and D_6 used in the present study are written as (Durran 1999):

$$D_4 = \gamma_4(-\phi_{i+2}+4\phi_{i+1}-6\phi_i+4\phi_{i-1}-\phi_{i-2}), \tag{A6}$$

$$D_6 = \gamma_6(\phi_{i+3}-6\phi_{i+2}+15\phi_{i-1}-20\phi_i+15\phi_{i-1}-6\phi_{i-2}+\phi_{i-3}), \tag{A7}$$

where, γ_4 and γ_6 are constant. That means the coefficient is not a function of the Courant number, in contrast to the implicit diffusion.

Manuscript received 11 August 2005, accepted 24 September 2005
SOLA: http://www.jstage.jst.go.jp/browse/sola/